

Characterization of DC current sensors with AC distortion for railway applications

Helko E. van den Brom, *Senior Member, IEEE*, Ronald van Leeuwen, and Ralph Hornecker

Abstract—To assess the reliability of DC energy measurement equipment on board trains, a setup was developed to characterize current transducers under realistic operating conditions. The operating principle is based on a current ratio measurement technique. The reference sensor is a high-precision zero-flux current transducer in combination with a broadband high-precision current shunt. The influence of AC distortion on this reference sensor was found to be within a few parts in 10^6 using an initial version of the setup, in which AC distortion was applied through a separate winding.

A revised version of the setup employs a programmable electronic load to apply dynamic currents up to 600 A. The setup was used to characterize a $100\ \mu\Omega$ high-current shunt resistor. The effect of dissipative heating on the DC transresistance error was around 0.03 %, with a settling time of about half an hour. The short-term intrinsic current dependence was also around 0.03 %. The effect of AC distortion was within a few parts in 10^6 . The intrinsic current dependence and the onset of the heating effect were also observed when exposing the sensor to a dynamic current profile that was recorded during a trip between two successive underground train stations on Metro de Madrid.

These results demonstrate that the setup described in this paper is very effective for characterizing DC current sensors for practical railway applications. Future work will concentrate on even more demanding current signals, such as chopped signals, and on other types of sensors and measurement systems.

Index Terms—Current measurement, current sensors, current transducers, measurement standards, measurement techniques, measurement uncertainty, precision measurements

I. INTRODUCTION

MARKET liberalization in railway transportation and the EU target of 50 % reduction of CO₂ emission by 2030 have set the need to accurately measure the energy consumption of individual trains. In railway systems, energy reduction can be realized by different means, such as regenerative braking, energy-efficient driving, reduction of traction losses, optimization of comfort functions, energy metering, smart power management and renewable energy micro-generation [1]. In all cases, accurate and reliable measurement of the amount of consumed, regenerated or stored energy is essential to quantify the actual reduction obtained.

European legislation requires that energy billing is based on measurement equipment on board trains by 2019 [2]. However,

due to harsh operating conditions such as arcing caused by non-ideal pantograph to overhead line contacts, extreme temperatures, and rapid acceleration and deceleration of the train, accurately measuring the current on-board trains is challenging. These harsh conditions create all kinds of electrical distortion influencing the measurement of electrical parameters on board trains.

The so-called energy measurement function (EMF) that should be implemented on board trains provides the measurement of the consumed and regenerated energy of a traction unit, as set out in [3]. The EMF consists of a voltage measurement function, a current measurement function and an energy calculation function. The voltage and current measurement functions include voltage and current transducers, respectively, as well as data-acquisition units. This paper focuses on the current measurement function for DC traction supply systems, that measures the DC current taken from and returned to the contact line system.

To verify and test current measuring equipment under realistic operating conditions as described above, a traceable measurement setup is developed to calibrate and characterize DC current sensors, or complete DC current measurement chains, under adjustable non-ideal conditions. Using this setup, non-ideal operating conditions can be simulated for railway applications, but also for other electrical systems used in transportation, such as for aircraft, ship propulsion or road vehicles.

Literature shows that monitoring of dynamic and highly distorted signals for AC or DC high-current applications has been investigated before (see, e.g., Refs. [4]-[7]). Nevertheless, no reference setup has been developed to provide traceability to international measurement standards for calibrations of the equipment used to measure such dynamic and distorted signals. Until now, traceable calibration systems for high-current measurement systems have only been presented for static signals (see, e.g., Refs. [8],[9]). For example, work on a testbed like the system described in this paper, which has been performed in parallel recently [6], does not show traceability of the reference current sensor under distorted conditions.

In previous work [10], a setup was described comparing two transducers measuring the same DC current, whereas one was exposed to a superimposed AC ripple distortion as well. In this paper we explain how the results are used to extend the setup to include more general non-ideal signals. The operating principle of the setup is explained, and its capabilities are demonstrated.

Manuscript received July 10, 2018. The research leading to the results described in this paper is performed within the 16ENG04 MyRailS project of the European Metrology Programme for Innovation and Research (EMPIR). The EMPIR initiative is co-funded by the European Union's Horizon 2020

research and innovation programme and the EMPIR participating states, including the Dutch Ministry of Economic Affairs and Climate Policy.

The authors are with VSL, Dutch Metrology Institute, P.O. Box 654, 2600AR Delft, The Netherlands (email: hvdbrom@vsl.nl).

Measurement results are presented characterizing a DC high-current shunt by means of direct comparison to a high-precision reference sensor.

II. CURRENT SENSORS

A. Types of current sensors

Two types of current sensors can be distinguished. The first type of sensor converts current to voltage, such as for example a current shunt for DC systems, or a Rogowski coil for AC systems. For these types of sensors, the transresistance or transimpedance value is the relevant parameter to be determined, defined as the ratio between the output voltage and the input current for DC or AC systems, respectively.

The second type of sensor converts a high input current to a much lower output current, such as for example a zero-flux current transducer [11] with current output for DC systems, or a current transformer for AC systems. For these types of sensors, the current ratio between input (or primary) current and output (or secondary) current is the relevant parameter to be determined. For these current-to-current transducers, an auxiliary high-precision current shunt can be used to convert the secondary current to voltage to be able to perform accurate measurements, or for direct comparison to current-to-voltage sensors. For simplicity, in this paper the combination of a current-to-current sensor and an auxiliary current shunt will be considered a current-to-voltage sensor.

B. Definition of the measurand

In this paper, the error is the deviation from the nominal value of the current ratio or transresistance, expressed as a relative value with respect to the nominal value. For a current-to-current sensor that converts a primary current I_p to a secondary current I_s , the current ratio error is defined as

$$\varepsilon = \frac{n \cdot I_s}{I_p} - 1, \quad (1)$$

where n is the nominal current ratio of the current sensor. The transresistance error of a current-to-voltage sensor, that converts an input current I_{in} to an output voltage V_{out} , is defined as

$$\varepsilon = \frac{V_{out}}{R_{nom} \cdot I_{in}} - 1, \quad (2)$$

where R_{nom} is the nominal transresistance value of the sensor.

In case of a current-to-voltage sensor that is compared to a current-to-current sensor, the same input or primary current I_{in} or I_p is sent through both sensors in series. Hence, from the definitions (1) and (2) one can derive that the error of the device under test (DUT), ε_{dut} , can be expressed in terms of the ratio of the two measured secondary currents I_s^{ref} and I_s^{dut} or output voltages V_{out}^{ref} and V_{out}^{dut} , the nominal current ratios of the reference sensor and the sensor under test n_{ref} and n_{dut} or the nominal transresistance values R_{nom}^{ref} and R_{nom}^{dut} , and the error of the reference sensor, ε_{ref} . For the situation described in this paper, in which a current-to-voltage sensor is compared to a current-to-current sensor, the corresponding equation reads

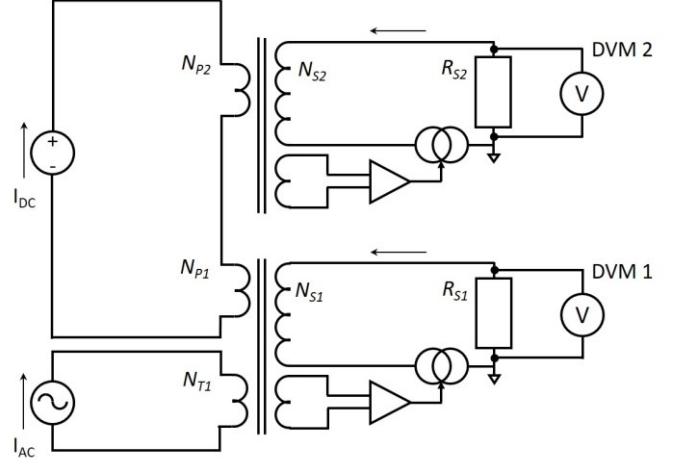


Fig. 1: Schematic of the initial measurement setup to compare two current sensors, labeled 1 and 2, at a DC current I_{DC} with AC distortion I_{AC} . Both sensors consist of a zero-flux current transducer, with N_P -turns primary winding and N_S -turns secondary winding, in combination with an auxiliary broadband high-precision shunt resistor (R_S). The AC distortion is applied through a separate N_T -turns primary winding. The output voltage of both sensors is measured using a high-precision digital voltmeter (DVM).

$$\varepsilon_{dut} = 1 - n_{ref} \cdot R_{nom}^{dut} \cdot \frac{I_s^{ref}}{V_{out}^{dut}} + \varepsilon_{ref}, \quad (3)$$

where the equality holds up to first order in the ratio errors. Hence, the transresistance error of the sensor under test can be read directly from the measured ratio of the secondary current and output voltage after a simple correction for the ratio error of the reference sensor. Note that (3) can be rewritten as

$$\varepsilon_{dut} = 1 - \frac{R_{nom}^{dut}}{R_{nom}^{ref}} \cdot \frac{V_{out}^{ref}}{V_{out}^{dut}} + \varepsilon_{ref}, \quad (4)$$

where now the combination of the current-to-current reference sensor and the auxiliary current shunt resistor R_{aux} is considered a current-to-voltage sensor having a transresistance equal to $R_{nom}^{ref} = R_{aux} / n_{ref}$.

III. MEASUREMENT SETUP FOR STATIC SIGNALS

A. Principle of operation

The basis of the measurement setup to characterize DC current sensors under distorted operating conditions lies in a current ratio measurement technique initially developed for comparing AC current transformers [8]. The operating principle of the setup is to compare the sensor under test to a reference sensor that is calibrated using a primary reference setup [9] and therefore traceable to international measurement standards. When the two sensors are connected in series to measure the same input current, the ratio of their output voltages can be used to determine the transresistance error of the sensor under test by means of equation (4). The harsh operating conditions can be mimicked by applying various non-ideal test signals.

In the initial version of the setup, only static test signals can be applied, composed of a DC current with or without AC distortion [10]. Furthermore, the sensor under test needs to

contain a zero-flux current transducer when AC distortion is applied. The corresponding schematic is shown in Fig. 1. The DC primary current is generated by means of a 100 A DC current source and is applied to the primary winding of the two sensors to be compared. The AC distortion is induced using a separate winding through the sensor under test.

B. Sampling ratio measurements

The ratio of the output voltages of the two sensors to be compared is measured using two high-precision digital voltmeters (DVM), either in DC voltage mode for DC voltages, or in sampling mode using an asynchronous sampling technique [12] when measuring AC distorted signals.

For AC distorted signals the DC component is defined as the zero-frequency component of the Fourier spectrum, which is equal to the average of all samples in the sampling time window. To avoid spectral leakage and thus low-frequency AC modulation of the DC component and measurement errors, the signal is resampled using spline interpolation at a rate that is an integer multiple of the repetition rate of the AC distortion waveform.

When using the asynchronous sampling technique, the aperture time of the sampling voltmeters used is set to 100 μ s with a sampling rate of 8 kS/s, taking 12000 samples in a single reading using a moving average of 10 readings. In DC voltage mode, 3 measurements are performed per second.

Using asynchronous sampling, the voltage ratio can be determined with an accuracy of better than 2 parts in 10^6 , which is limited by the linearity of the voltmeters [8].

C. Current sensors to be compared

The sensor under test in this initial setup, labeled 1 in Fig. 1, is in fact meant to be used as reference sensor in a revised setup as described in the next chapter, allowing for different distortion signals and other types of transducers. This sensor is a high-precision zero-flux current transducer with a nominal ratio of 1500:1, a 900 A maximum primary current and 1 MHz bandwidth, in combination with a broadband 1 A current shunt to convert the output current to voltage. The DC current ratio of this zero-flux current transducer and the intrinsic current dependence over a wide range of input currents were determined with an accuracy of 1 μ A/A ($k=2$) using a direct current comparator bridge that is originally designed for high-current low-resistance calibrations [9]. The broadband 1 A current shunt was designed to have very low AC-DC difference for frequencies up to 100 kHz [13] and calibrated at DC using standard resistance calibration techniques with an accuracy of better than 1 $\mu\Omega/\Omega$ ($k=2$). The high bandwidth of both zero-flux current transducer and current shunt are necessary to allow for dynamic current signals, as further discussed in Section V.

As a second sensor, labeled 2 in Fig. 1, a similar zero-flux current transducer is used with a nominal ratio of 600:1 and 60 A maximum primary current, in combination with a broadband high-precision 100 mA current shunt. This zero-flux current transducer is stable within the time of measurement, but only accurate to the level of 200 μ V/V. This sensor is used as a stable reference for this measurement to verify the behavior of the first transducer under AC distortion.

The major difference in nominal operating currents of the two transducers is largely compensated by looping the DC primary

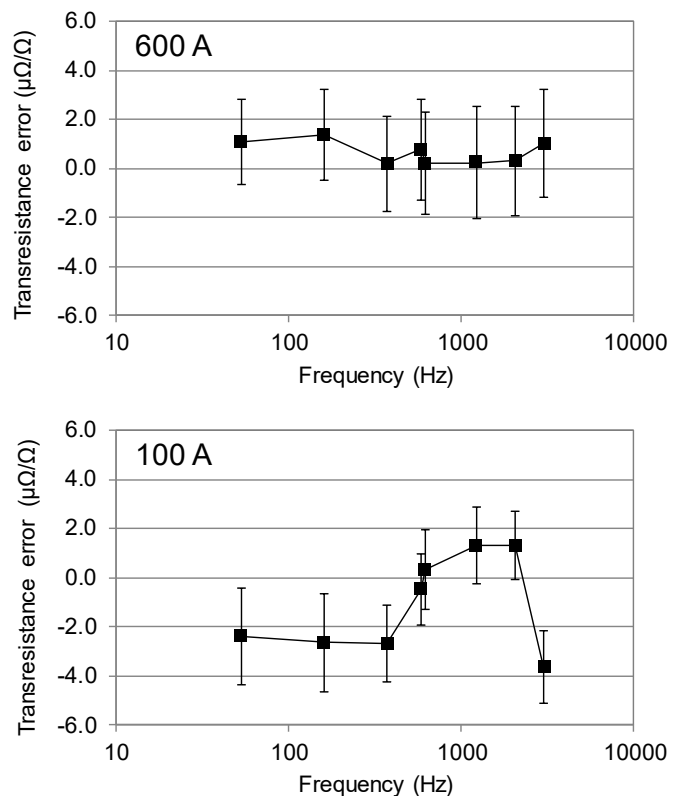


Fig. 2. Relative effect of an AC distortion current on the DC output voltage of the reference transducer for a DC current of 600 A (upper curve) and 100 A (lower curve). The same AC distortion current is applied in the two cases.

conductor 10 times through the primary winding of the first transducer. DC currents up to 60 A are then sent through the 10-turns primary winding of the latter transducer (effectively resulting in primary DC currents up to 600 A) and through the single-turn winding of the second transducer.

The AC distortion, with effective rms magnitudes up to 24 A, is applied exclusively to the first transducer by means of a separate 24-turns winding. An isolation transformer is used to avoid possible DC offsets in the AC circuit that would not be sensed by the second transducer, thus erroneously changing the ratio of the DC output readings.

IV. RESULTS OF THE SETUP FOR STATIC SIGNALS

For the setup indicated in Fig. 1, AC distortion signals were applied with rms magnitudes of 24 A for frequencies up to 1 kHz, whereas for higher frequencies the rms magnitude was decreased to 8 A at 3 kHz to satisfy the compliance limit of the transconductance amplifier used to generate the distortion current. Measurements were performed at different frequencies for effective DC currents of 600 A and 100 A. The same AC distortion current is used in both cases, such that for the DC current of 600 A the relative level of distortion is 6 times lower than for 100 A (i.e., 4 % as compared to 24 %, respectively).

The transresistance error due to the AC distortion current on the DC output voltage of the reference transducer is presented in Fig. 2. The error bars show the standard deviation of the mean when using the moving average of the individual readings. When applying a DC current of 600 A, the AC distortion seems to have negligible effect, as can be seen in the

Table I: Uncertainty budget of the reference sensor at 600 A DC when used under distorted conditions.

Uncertainty component	Uncertainty contribution ($\mu\Omega/\Omega$)	k-factor	Standard uncertainty ($\mu\Omega/\Omega$)
Primary standard	1.0	2	0.5
Effect AC distortion	5.0	$\sqrt{3}$	2.9
Voltmeter ratio	2.0	$\sqrt{3}$	1.2
Standard deviation	2.5	1	2.5
Total (k=2)	6.5	2	3.3

upper graph in Fig. 2. When reducing the applied DC current to 100 A and keeping the same amplitude of the AC distortion, however, a minor effect can be observed in the lower graph, though without a clear trend.

From these observations, it can be concluded that the influence of severe AC distortion on the DC output reading of the reference transducer is within 5 parts in 10^6 .

The total uncertainty of the reference transducer when used under distorted conditions is determined by the DC calibration using the primary reference setup [9], the influence of the AC distortion as described in this Section, the accuracy of the voltmeter ratio, and the standard deviation of the measurements (type A uncertainty). The total uncertainty budget for a DC input current of 600 A is shown in Table I; the total expanded uncertainty is $6.5 \mu\Omega/\Omega$ (k=2). For DC currents down to 100 A the total uncertainty will be slightly larger, but still well within $10 \mu\Omega/\Omega$ (k=2).

V. MEASUREMENT SETUP FOR DYNAMIC SIGNALS

A. Principle of operation

The idea of the improved setup is to be able to measure current sensors not exclusively based on zero-flux current transducers. At the same time, by means of this setup one should be able to apply a broader range of test signals. The operating principle and the sampling technique is similar to the initial setup described in Section III.

Fig. 3 shows the schematic of the revised measurement setup. The DC primary current I_p , sent through the two sensors to be compared, is generated by means of a 900 A high-power DC current source and modulated using a programmable DC electronic load Z_{load} that is connected in series. The load can be programmed to simulate various load profiles with unipolar currents up to 600 A with frequency components up to 20 kHz. Examples relevant for railway applications are DC current with AC distortion (ripple), DC current varying with time, or user-defined waveforms. In this way, the device under test can be characterized under conditions that resemble normal operation conditions for the current sensor, found in traction units or in other electrical systems in transportation applications.

Please note that by adapting the setup, any combination of current-to-current and current-to-voltage sensors can be compared by adding or removing proper auxiliary high-precision shunts. In fact, even complete current measuring systems including readout ammeter or voltmeter can be characterized when leaving out the second DVM.



Fig. 3: Schematic of the measurement setup to characterize a DC current sensor using dynamic current signals. The device under test here is a high-current shunt (R_{dut}). The reference current sensor consists of a zero-flux current sensor in combination with an auxiliary high-precision shunt resistor (R_{aux}).

B. Current sensors to be compared

In this paper, the working principle of the revised measurement setup will be demonstrated using the setup shown in Fig. 3. The current sensor under test in this case is a high-current shunt with resistance R_{dut} of nominally $100 \mu\Omega$, designed for operation for currents up to 300 A and equipped with an active cooling fan.

The reference current sensor in the revised setup is the combined zero-flux current transducer and auxiliary high-precision current shunt R_{aux} investigated in the previous chapter. Since in this study the typical currents are a few times smaller than the 900 A maximum input, a two-turn primary winding is used to increase the effective input current to 600 A when applying 300 A to the shunt under test, for two reasons, i.e., for demonstrating operation of the setup for currents up to 600 A, and for increasing the sensitivity of the sensor.

VI. RESULTS OF THE SETUP FOR DYNAMIC SIGNALS

Various measurements have been performed to characterize the current shunt under test, as described more extensively in a separate publication [14]. These measurements were designed to isolate the influence of the stability of the shunt, intrinsic current dependence, response to dynamic loading, and the effect of AC distortion. Specific tests for other applications, such as using chopped signals, can be performed as well.

To calibrate the transresistance value of the current shunt under test and to investigate the possible effect of self-heating, the transresistance error is measured at a DC current of 270 A. As can be seen in Fig. 4, after settling for about half an hour, the final value is about 0.03 % lower than the value found directly after switching on the current. By investigating the corresponding individual current recordings of the two sensors, it is observed that the drift is caused by the shunt, whereas the reference sensor shows no drift at all, as expected. Note that this effect of self-heating is adjacent to the influence of the external temperature, which is less than 5 parts in 10^6 per degree Celsius according to the manufacturer specifications, corresponding to another 0.03 % for a realistic temperature range between -20°C and $+40^\circ\text{C}$.

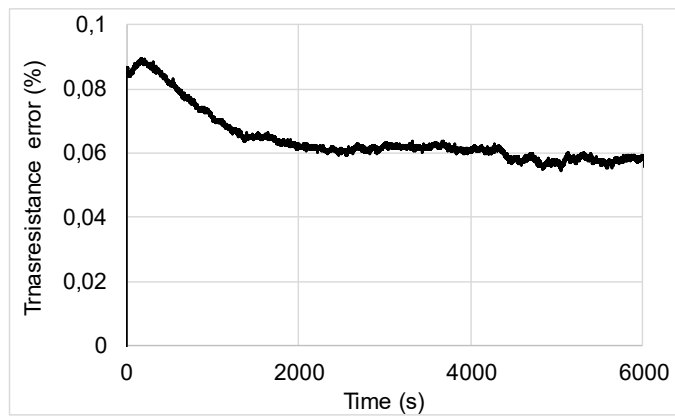


Fig. 4: Measured transresistance error of the current shunt under test as a function of time after applying a static DC current of 270 A.

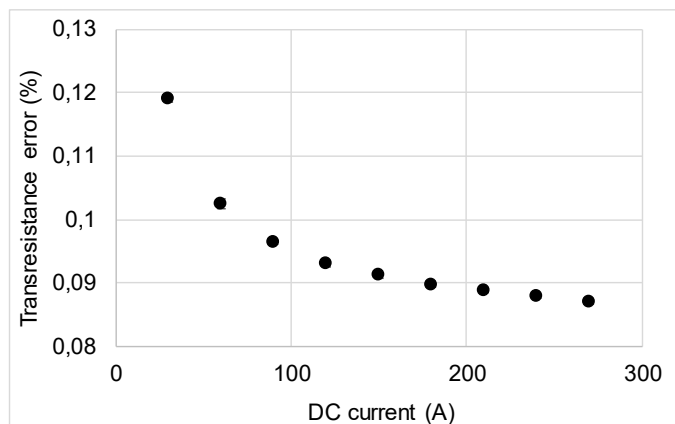


Fig. 5: Measured transresistance error of the current shunt under test as a function of applied DC current for the chopped waveform described in the text.

In a separate measurement, the current dependence caused by intrinsic properties of the shunt other than dissipation has been determined. To do so, the electronic load is programmed with a chopped current profile in which the current is alternately switched on for 5 seconds and switched off for 10 seconds. The current level is increased by 30 A with each step to a maximum of 270 A. The whole sequence is repeated 5 times, with several minutes in between. From the results, shown in Fig. 5, it can be seen that the transresistance error increases with decreasing current. The largest error deviates by 0.03 % from the smallest error measured at the largest current, which resembles the value obtained before the heating sets in (as can be read from Fig. 4). The standard deviation of the measurements, shown as error bars in the figure, is typically a few parts per million only, which is not noticeable in the figure.

To mimic realistic operating conditions, a waveform is used that resembles the power consumption of a real traction unit. For this measurement we used current data recorded at the pantograph of a traction unit traveling between successive underground stations of Metro de Madrid. The corresponding loading patterns are programmed into the memory of the electronic load. Both sensors can follow the dynamic behavior of the current. As expected, Fig. 6 reveals that the measurements resemble the behavior observed in Fig. 5, that is, the error increases with decreasing current. The onset of the heating effect can also be observed between 33 s and 43 s, in

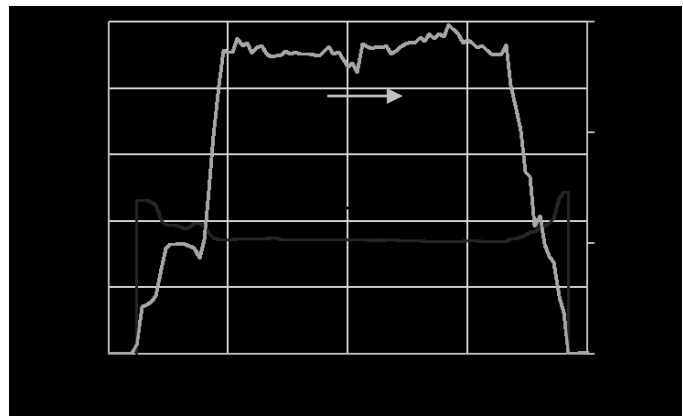


Fig. 6: Measured transresistance error of the current shunt under test (black line, left axis) during a simulated segment of a trip of an underground traction unit with the corresponding DC current applied (grey line, right axis).

which the applied current is approximately constant whereas the transresistance error shows a minor decrease. Hence, the effect of the dynamics of the current waveform are covered by the effect of dissipation and the intrinsic current dependence already investigated. Alternatively, one might argue that when calibrating the current shunt under realistic dynamic conditions, the effect of dissipation and intrinsic current dependence are included. Note that this observation can be considered a cross-check of the ability of the reference sensor for correctly measuring dynamic DC signals.

To determine the effect of AC distortion on the current shunt, the electronic load is programmed with DC signals with and without additional AC component. From the measurements described in the previous section it was concluded that the sensor used as reference in the revised measurement setup is not influenced by AC distortions to within a few parts in 10^6 . From the measurements described here it was found that, to within the error bars representing the standard deviation of the measurements of a few parts in 10^6 , the current shunt under test shows no dependence on the frequency or amplitude of the AC distortion either.

The total uncertainty of the transresistance ratio of the current shunt under test when used under realistic conditions is determined by the reference sensor (Table I), dissipation, intrinsic current dependence, the influence of AC distortion, the accuracy of the voltmeter ratio, the temperature dependence, and the standard deviation of the measurements (type A uncertainty). The total uncertainty budget for a DC input current of 270 A is shown in Table II; the total expanded uncertainty is 0.05 % ($k=2$). For DC currents down to 30 A the total uncertainty will be similar. Note that if this current shunt is used in real railway applications, another 0.03 % (rectangular distribution) needs to be added due to its temperature coefficient of resistance.

VII. SUMMARY AND CONCLUSIONS

A measurement setup has been realized to characterize the DC output error of current sensors under realistic operating conditions for railway applications. In the initial setup, suitable only for static signals and for sensors containing zero-flux current transducers, an AC distortion was applied through a separate winding. This setup was used mainly to prove that the

Table II: Uncertainty budget of the current shunt under test at 270 A DC when used under distorted conditions.

Uncertainty component	Uncertainty contribution (%)	k-factor	Standard uncertainty (%)
Reference sensor	0.001	2	0.001
Dissipation	0.030	$\sqrt{3}$	0.017
Current dependence	0.030	$\sqrt{3}$	0.017
AC distortion	0.001	$\sqrt{3}$	0.001
Voltmeter ratio	0.000	$\sqrt{3}$	0.000
Standard deviation	0.001	1	0.001
Total (k=2)	0.050	2	0.025

reference sensor used in a revised version of the setup, based on a programmable electronic load, was immune to AC distortion to within a few parts in 10^6 . The total uncertainty of the reference sensor was found to be smaller than $10 \mu\Omega/\Omega$ (k=2).

The revised setup employs a programmable electronic load, which makes it suitable to apply dynamic signals. The setup can deal with different types of current sensors or even complete current measurement systems. The current sensor under test is compared to a reference sensor, consisting of a high-precision zero-flux current transducer in combination with a broadband high-precision shunt resistor. Distorted operating conditions can be simulated for currents up to 600 A.

For the specific sensor under test in this paper, a $100 \mu\Omega$ high-current shunt designed for measurements with currents up to 300 A, the longer-term effect of dissipative heating was found to be around 0.03 % for an applied DC current of 270 A. The short-term intrinsic current dependence was found to be around 0.03 % as well when comparing the error at currents down to 30 A to the error determined at 270 A. The effect of AC distortion on the DC transresistance error was found to be within a few parts in 10^6 , which is negligible when comparing to the other effects. The intrinsic current dependence and the onset of the heating effect were also observed when exposing the sensor to a dynamic current profile that was recorded during a trip between two successive underground train stations from Metro de Madrid. The total uncertainty of the reference sensor was found to be smaller than 0.05 % (k=2). However, it should be noted that the temperature in the laboratory was $(23.0 \pm 0.5)^\circ\text{C}$ and the shunt was equipped with a cooling fan, whereas in practical railway applications the temperature can vary between, say, -20°C and $+40^\circ\text{C}$, and active cooling of the shunt might be absent or less effective.

The observed transresistance error of the high-current shunt investigated in this paper was around 0.10 %. The accuracy of the total energy measurement function of railway traction units, including current and voltage measurement and energy calculation, needs to be on the order of 0.2 % to 1 % [3]. Hence, when taking the uncertainty into account as well, the shunt under investigation would be just satisfactory for most metering applications on-board trains.

The effect of AC distortion on the error of the shunt is shown to be negligible. It should be noted, however, that AC ripple might still influence the complete current measurement system. Modulation and spectral leakage might disturb the reading of the meter if it is not configured correctly. However, in this paper

the focus is on current sensors only and the investigation of complete current measuring systems is left for future work.

From the results presented here, we conclude that the setup described in this paper is very useful for characterizing DC current sensors for practical railway applications under realistic distortion conditions. Whereas in this paper the emphasis is on traceability of the measurements including uncertainty analysis, details on the use of the setup for practical applications are described more extensively elsewhere [14]. Future work will concentrate on even more demanding current signals such as chopped signals, and on the characterization of other types of transducers and complete current measurement systems.

ACKNOWLEDGMENT

We thank Jorge Quintana Fernández and Fabio Balic for providing us with the current profiles measured in the underground traction unit of Metro de Madrid and for valuable discussions.

REFERENCES

- [1] Arturo González-Gil, Roberto Palacin, P. Batty, and Jonathan Powell, "A systems approach to reduce urban rail energy consumption", *Energy Convers. Manage.*, vol. 80, pp. 509–524, April 2014.
- [2] Commission Regulation (EU) No 1301/2014 of 18 November 2014 on the technical specifications for interoperability relating to the energy subsystem of the rail system in the Union.
- [3] EN 50463-2:2012, "Railway applications - Energy measurement on board trains - Part 2: Energy measuring".
- [4] A. Cataliotti, D. Di Cara, A. E. Emanuel, and S. Nuccio, "A Novel Approach to Current Transformer Characterization in the Presence of Harmonic Distortion," *IEEE Transactions on Instrumentation and Measurement*, vol. 58, no. 5, pp. 1446-1453, May 2009
- [5] A.P.J. van Deursen, P.A.A.F. Wouters, H.W.M. Smulders, and J.B.M. van Waes, "EMC measurements in railway power systems", *Proceedings of the 2012 International Symposium on Electromagnetic Compatibility (EMC Europe)*, Rome, Italy, Sept. 2012
- [6] G. Crotti, D. Giordano, A. Delle Fernine, D. Gallo, C. Landi, M. Luiso, "A Testbed for Static and Dynamic Characterization of DC Voltage and Current Transducers," 9th IEEE International Workshop on Applied Measurements for Power Systems (AMPS 2018), Bologna, Italy, Sept. 2018
- [7] G. Crotti, D. Giordano, P. Roccatto, A. Delle Fernine, D. Gallo, C. Landi, and M. Luiso, and A. Mariscotti, "Pantograph-to-OHL Arc: Conducted Effects in DC Railway Supply System", 9th IEEE International Workshop on Applied Measurements for Power Systems (AMPS 2018), Bologna, Italy, Sept. 2018
- [8] H. E. van den Brom, G. Rietveld, and E. So, "Sampling Current Ratio Measurement System for Calibration of Current Sensors up to 10 kA with $5 \cdot 10^{-6}$ Uncertainty", *IEEE Trans. Instr. Meas.*, vol. 64, no. 6, pp. 1685–1691, June 2015.
- [9] G. Rietveld, J. H. N. van der Beek, and E. Houtzager, "Accurate DC Current Ratio Measurements for Primary Currents up to 600 A", *IEEE Trans. Instr. Meas.*, vol. 64, no. 11, pp. 3055–3061, Nov. 2015.
- [10] H. E. van den Brom, R. van Leeuwen, and R. Hornecker, "Characterization of a reference DC current sensor with AC distortion for railway applications", *Conf. Prec. Elec. Meas. Digest*, Paris, France, 8-13 July 2018.
- [11] H. C. Appelo, M. Groenenboom, and J. Lisser, "The Zero-Flux DC Current Transformer – a High Precision Bipolar Wide-Band

Measuring Device”, *IEEE Trans. Nucl. Sci.*, vol. 24, no. 3, pp. 1810–1811, June 1977.

- [12] W. G. K. Ihlenfeld and M. Seckelmann, “Simple algorithm for sampling synchronization of ADCs,” *IEEE Trans. Instrum. Meas.*, vol. 58, no. 4, pp. 781–785, Apr. 2009.
- [13] K. Lind, T. Sorsdal, and H. Slinde, “Design, Modeling, and Verification of High-Performance AC–DC Current Shunts from Inexpensive Components”, *IEEE Trans. Instr. Meas.*, vol. 57, no. 1, pp. 176–181, Jan. 2008.
- [14] H. E. van den Brom, R. van Leeuwen, and R. Hornecker, “Characterization of DC current sensors under distorted conditions for railway applications”, *ESARS-ITEC Conf. Digest*, Nottingham, UK, 7-9 Nov. 2018.



Helko E. van den Brom (M’14–SM’15) was born in Utrecht, the Netherlands, in 1971. He received the M.Sc. degree in theoretical solid-state physics from Utrecht University in 1995, and the Ph.D. degree in experimental solid-state physics from Leiden University, the Netherlands, in 2000.

In 2000, he joined VSL, Delft, the Netherlands, where he started working on the development of Josephson and SET based electrical quantum standards. At present, as a principle scientist his current research interests are in power quality, high-current transducers, sampling systems, and AC Josephson voltage standards.

Dr. Van den Brom is a member of the Dutch Physical Society (NNV), technical assessor for the Dutch Accreditation Council (RvA), contact person for VSL in the technical committee of electricity and magnetism (TCEM) and the subcommittee of DC and quantum electrical measurements of the European Association of National Metrology Institutes (EURAMET). He was a recipient of the best Ph.D. paper award of the Dutch Journal of Physics (NTvN) in 2000.

Ronald van Leeuwen was born in Nieuwerkerk aan den IJssel in the Netherlands. He received the M.Sc. degree in applied physics from Delft University of Technology in 2010, and the Ph.D. degree in applied physics from Delft University of Technology in 2015.

In 2017, he joined VSL, Delft, the Netherlands, where he started working on development of measurement techniques for high current transducers. Furthermore, he is also involved in the development of new techniques for testing of static electricity meters.

Dr. Van Leeuwen won the 2014 NEVAC prize (Dutch vacuum society) for best scientific article, Title: “Luisteren naar nanodrum met atomaire dikte”.



Ralph Hornecker was born in Endingen, Germany, in 1988. He received the B.Eng. degree in electronics from University of Applied Sciences Aschaffenburg, Aschaffenburg, Germany in 2017.

After his studies, in 2017, he joined VSL, Delft, the Netherlands, where he specialized in Power Quality and low-frequency high-current measurement. Furthermore, he became involved in the

development of a quantum alternating-current voltage standard.